Contribution of low-salinity water to sea surface warming of the East China Sea in the summer of 2016

Jae-Hong Moon[a], Taekyun Kim[b,*], Young Baek Son[c], Ji-Seok Hong[a], Joon-Ho Lee[a], Pil-Hun Chang[d], Soo-Kang Kim[e]

[a] Department of Earth and Marine Sciences, College of Ocean Sciences, Jeju National University, Jeju 63243, Republic of Korea
[b] Unit of Ice Sheet and Sea Level Changes, Korea Polar Research Institute, Incheon, Republic of Korea
[c] Korea Institute of Ocean Science and Technology, Republic of Korea
[d] Earth System Research Division, National Institute of Meteorological Sciences, Republic of Korea
[e] Ocean and Fisheries Research Institute, Jeju, Republic of Korea

ARTICLE INFO

ABSTRACT

Substantial low-salinity water (< 26 psu) was observed in the northern East China Sea (ECS) in the summer of 2016, resulting in significant warming (~2 °C) of sea surface temperature (SST) over the freshening area compared to normal year. By analyzing the ship-based hydrographic datasets, horizontal temperature and salinity distributions tracked by a wave glider, and results from a regional ocean model, this study examined the spatiotemporal behavior of low-salinity water over the northern ECS and its contribution to SST warming during summer. The observations revealed that a large amount of the freshwater originating from the Changjiang significantly stratified the surface layer above the top of the thermocline, resulting in a shallow mixed layer (ML) in which significant warming was found. The shallow ML led to a barrier layer formation between the ML and the layer below the ML that can enhance SST warming by restricting heat exchanges between the surface and the thermocline. Our model successfully captured the strong surface warming over the northern ECS observed during the summer of 2016, which corresponded to significant areas of surface freshening. The model-data comparisons demonstrate that the salinity-stratified ML had a significant impact on the enhancement of barrier layer formation, leading to increased SST warming over the areas wherein surface freshening was robust.

1. Introduction

Increased solar heating during summers induces an increase in the sea surface temperatures (SST), which exerts a significant influence on weather conditions by affecting the formation of rain bands and local air temperatures in coastal regions (e.g., Gao et al., 2011; Lee et al., 2016). SST warming also can be influenced by the formation of a salinity-induced mixed layer (ML) above the thermocline. Fresh water that enters near the surface can lead to a shallow ML within the deep isothermal layer (IL), thereby resulting in a barrier layer (BL) between the base of the ML and the base of the IL (Sprintall and Tomczak, 1992). The BL separates the surface from the thermocline by impeding vertical heat exchange between the warm surface water and the cold thermocline below (Lukas and Lindstrom, 1991). This property of the BL can enhance SST warming by reducing the vertical exchange with the thermocline and by trapping heat from the atmosphere in shallow

salinity-stratified MLs (Foltz and McPhaden, 2009).

The summer hydrographic property in the northern East China Sea (ECS) is characterized not only by high SSTs but also by low surface salinity because of freshwater input from rivers. The Changjiang (also called the Yangtze River) is a significant source of freshwater for the ECS during summer when river discharges are large (Shen et al., 1998). The discharge from the Changjiang has a remarkable seasonal variation with the maximum value in July being 5–6 times higher than the minimum in January [Senjyu et al., 2006]. The arrival of enormous volumes of fresh water into the ECS forms a low-salinity water by mixing with saline ambient water (Lie et al., 2003), which is known as the Changjiang Diluted Water (CDW). The CDW contributes to substantial freshening of the surface layer over the northern shelf of the ECS, mostly spreading from the Changjiang mouth to the adjacent seas of Jeju Island, located about 450 km northeast from the river mouth. The northeastward extension of the CDW during summer may play an

---

important role in the BL formation associated with near-surface salinity stratification that can exert an influence on SST warming.

However, the impact of BLs on SST warming in the ECS has to date received little attention and few studies have reported on the relationship between SST and BL formation due to the CDW extension. Delcroix and Murtugudde (2002) showed that the CDW leads to sea surface warming in summer by comparing two comparative experiments with and without the Changjiang discharge (CD). However, they suggested that the effect of the BL on SST warming is not enhanced because advection of different regional temperatures prevents the formation of an IL below the ML. Moreover, a specific impact of the CDW on SST cooling was reported by Kako et al. (2016) who focused on the important role played by ocean currents in the SST reduction. By using a backward particle-tracking model, they noticed that summertime SST reduction in the ECS was considerably influenced by the CDW along the Chinese coast during the previous winter. In contrast, Park et al. (2011) emphasized a thermal response to the CD related to the BL formation in the Yellow Sea (YS) and ECS, using on sensitivity experiments that used a global ocean general circulation model. Despite these modeling efforts, no agreement has been reached on the role of the CDW in SST warming because of limited temporal and spatial *in situ* observation over the ECS.

According to recent satellite-based SST anomalies, abnormal SST warming of up to ~2 °C occurred in the northern ECS in the summer of 2016 (Fig. 1), a phenomenon rarely observed over the past decade, which caused severe damage to Korean fishing and aquaculture industries. This SST warming clearly appeared over the northern shelf of the ECS with a patchy structure of warming signals. This warming pattern matches the typical distribution of the low-salinity water

originating from the Changjiang, as presented by previous studies (Chang and Isobe, 2003; Lie et al., 2003; Moon et al., 2009, 2010, 2012; Hong et al., 2016). Considering the severe flooding that took place over the Changjiang area in the summer of 2016, it is reasonable to suspect that the CD-induced surface freshening may have contributed to the SST warming over the northern ECS through the BL process.

In this study, we examined how the CDW affected the abnormal SST warming that occurred over the northern shelf of the ECS during the summer of 2016 using ship-based hydrographic data, horizontal CTD profiles tracked by a wave glider, and comparative ocean modeling results. The observational data and model configurations are described in Section 2. In Section 3, we analyze several *in situ* temperature and salinity datasets and interpret the results in terms of the SST warming associated with surface freshening. We then discuss the model results in Section 4, focusing on the role of the CDW in the BL formation, resulting in the SST warming. A final summary and discussion are provided in Section 5.

2. Observational data and model descriptions

2.1. Observational data

Intensive *in situ* surveys and wave glider measurements were conducted in the northern shelf of the ECS during the summer of 2016. On July 22–25, 2016, CTD measurements along the north-south transect at 124.5°E were carried out by the Korea Meteorological Administration (KMA) RV *Gisang 1* (Fig. 2b). To obtain a synoptic pattern of low-salinity water, a hydrographic survey was also conducted by the Jeju National University (JNU) on four east-west lines between 124°E and
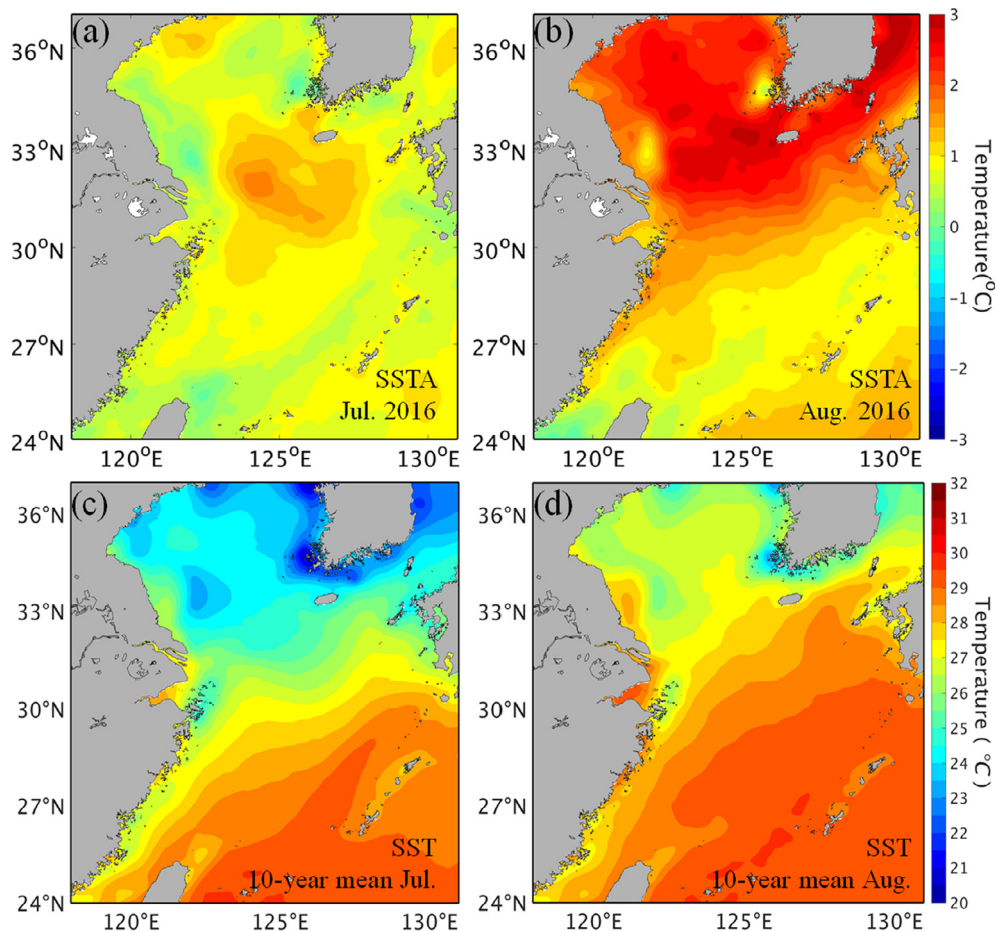
Fig. 1. Distributions of satellite-based SST anomalies over the ECS in (a) July and (b) August 2016, and long-term (2006–2016) mean SST in (c) July and (d) August from the Operational Sea Temperature and Sea Ice Analysis (OSTIA) product.
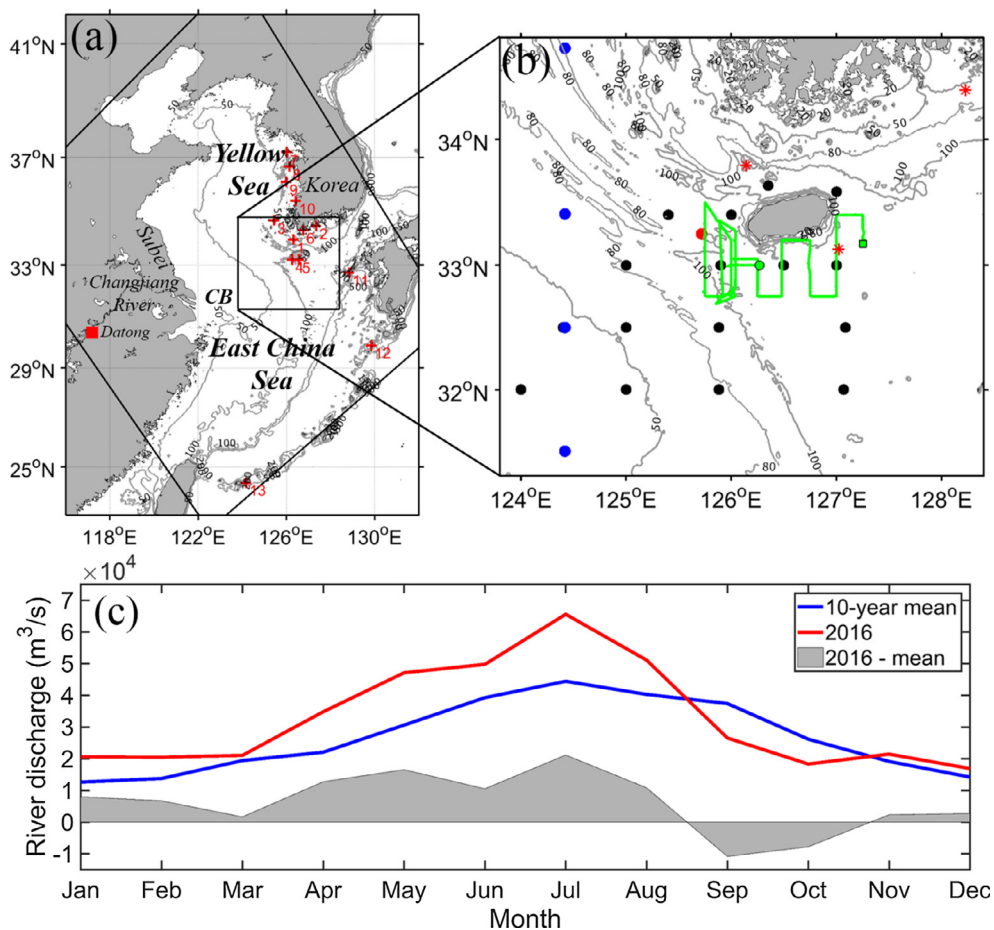
Fig. 2. (a) Model domain (rotated square box) and bathymetry (m) in the Yellow and East China Seas; red-cross symbols represent tide gauge stations. (b) Bathymetry of study areas; the blue, black, and red dots represent hydrographic stations compiled by KMA, JNU, and OFRI, respectively; red asterisk indicates the locations of ocean buoys and the green line indicates wave glider track from August 20 to September 20, 2016. (c) Climatological (blue) and monthly (red) discharge in 2016 from the Changjiang River; their difference is shaded in gray. (For interpretation of the references to colour in this figure legend, the reader is referred to the web version of this article.)
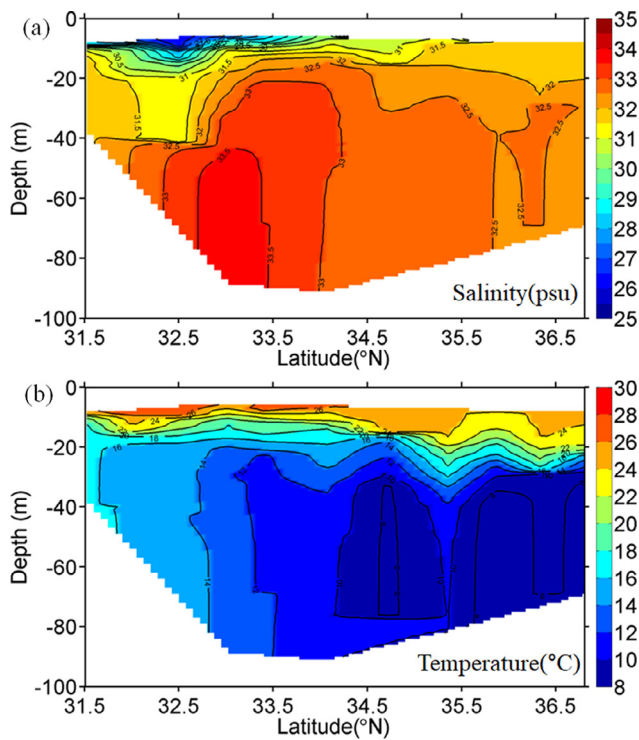
Fig. 3. Vertical sections of observed salinity and temperature along the north-south KMA line at 124.5°E on late July 2016.

127°E, 32°N and 33.5°N on August 16–19, 2016 (Fig. 2b) when the offshore extension of the CDW was fully developed over the northern ECS shelf. On August 17, 2016, an additional CTD measurement was made at a station near the west coast of Jeju Island (Fig. 2b) by the Ocean and Fisheries Research Institute (OFRI) to compare the vertical profiles with those observed in August 2012, when no readings below 29 psu were found. Temperature and salinity from SeaBird 19 Plus CTD (www.seabird.com) measurements were subsampled every 1 m by averaging the downcast data around each computation depth, with the calibration range ± 0.002 °C for temperature and ± 0.0003 S/m for conductivity.

To examine the spatial and temporal evolution of low-salinity water, we analyzed horizontal temperature and salinity data that were collected by a wave glider, which is an unmanned hybrid sea surface and underwater vehicle that comprises a submerged glider attached via a tether to a surface float (Daniel et al., 2011, Moh et al., 2018). Temperature and salinity data are continuously measured at a depth of 8 m by the temperature and salinity sensor mounted on the glider (i.e., Glider Payload CTD, GPCTD: Sea-Bird Scientific). The GPCTD is a modular, low-power profiling instrument with the high accuracy necessary for moored observatory sensors (Conductivity: calibration range ± 0.0003 S/m, Temperature: calibration range ± 0.002 °C, Pressure: calibration range ± 0.1% of full scale range). The SST can be measured by temperature sensor of glider-mounted ADCP at the surface. A wave glider was launched off the south coast of Jeju Island on August 15, 2016, to survey the characteristics of low-salinity water over the southwestern seas of Jeju Island. After an initial test period (August 15–20), the glider moved westward on August 21, 2016 (Fig. 2b), and then traveled northward and southward across the west sea of Jeju Island over several days, as shown by green lines in Fig. 2b. Thereafter, the glider followed a zigzag path to the east across the southern sea of
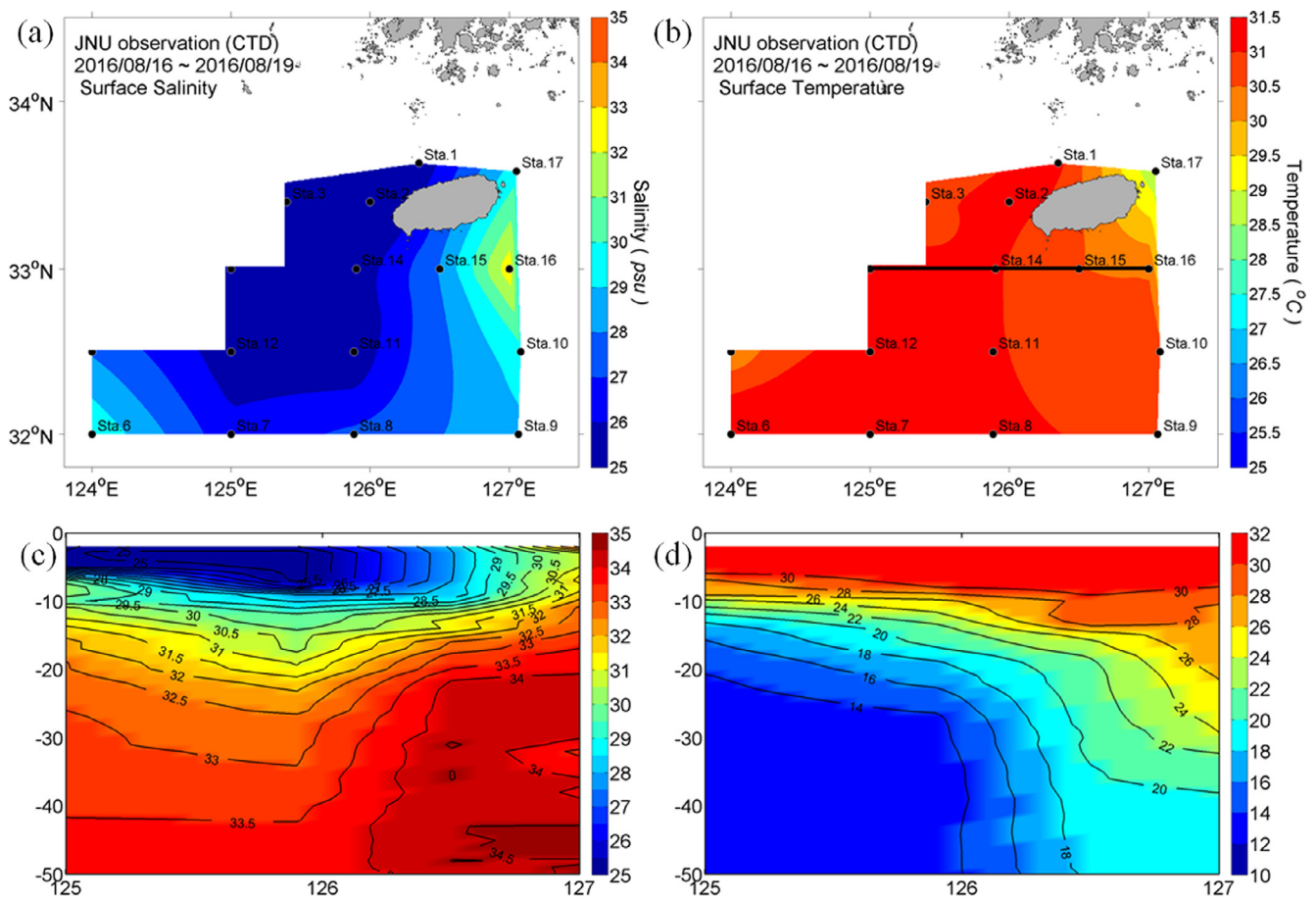
Fig. 4. (a, b) Horizontal distributions of salinity and temperature at 2 m depth observed by JNU on August 16–19, 2016. (c, d) Vertical sections of observed salinity and temperature along the east-west line at 33°N marked by black line.

Jeju Island. The horizontal temperature and salinity data were collected at 30-min intervals for 30 days by the Korea Institute of Ocean Science and Technology. To emphasize the characteristic features of low-salinity water, we analyzed the glider temperature and salinity data for the period of August 21–30, 2016, when the low-salinity water was obviously detected in the southwestern sea of Jeju Island.

2.2. Model configurations

We used the Regional Ocean Modeling System (ROMS: Shchepetkin and McWilliams, 2005; Haidvogel et al., 2008) in a regional configuration over the YS and ECS (Fig. 2a). The computational grid has an average horizontal resolution of 8 km with 20 vertical terrain-following layers. The bottom topography was extracted from the General Bathymetric Chart of the Oceans (GEBCO) 30 arc-second bathymetry (http://www.gebco.net/). The bottom stress was parameterized by a quadratic bottom friction law with a drag coefficient of 0.0025. The Generic Length Scale vertical mixing closure scheme using k-kl parameterization was used as a vertical mixing parameterization (Umlauf and Burchard, 2003; Warner et al., 2005).

The initial and open boundary conditions for the subtidal sea surface height and the momentum, temperature, and salinity were obtained from the daily mean global Hybrid Coordinate Ocean Model (Bleck, 2002, Chassignet et al., 2007) from January 1 to December 31, 2016. The formulations of the open boundary condition for the barotropic mode comprised the Chapman formulation (Chapman, 1985) for free surface and the modified Flather formulation for barotropic momentum (Marchesiello et al., 2001). The Clamped formulations for baroclinic momentum, temperature, and salinity were also applied

along with a sponge layer near the boundary. Real-time tides were considered using 10 tidal constituents (M2, S2, N2, K2, K1, O1, P1, Q1, Mf, Mm) derived from the TPXO (TOPEX/POSEIDON) 7-atlas for sea surface height and barotropic momentum along the open boundary conditions. The surface forcing obtained from the National Center for Environmental Prediction Final analysis (FNL) 6-hourly data for 2016 were used to compute the surface boundary conditions with the bulk formulation (Fairall et al., 1996). River forcing from Changjiang was included as a freshwater source in this model. The salt flux in the model was basically balanced by precipitation and evaporation, which is corrected by sea surface salinity climatology with 90 days relaxation time. The monthly average discharge from the Changjiang was obtained from the available data at the Datong hydrometric station for 2016 (Fig. 2c). The temperature value of the river outflow was given by the climatology of monthly surface temperature near the river mouth to minimize the effect of thermal difference between the freshwater and sea water temperature. In this study, two comparative model trials were designed to examine the SST response to a freshwater source: one with zero salinity and the other with 30 psu. It should be noted that the salinity value entering the model cell of the river outflow is different; however, the volume of the CD is the same for both the experiments. To highlight the summer responses, the salinity of 30 psu was imposed on the model after June 1, 2016. The comparison between these two experiments provides insight into sea surface warming as a direct thermal response to salinity-induced ML during summer.
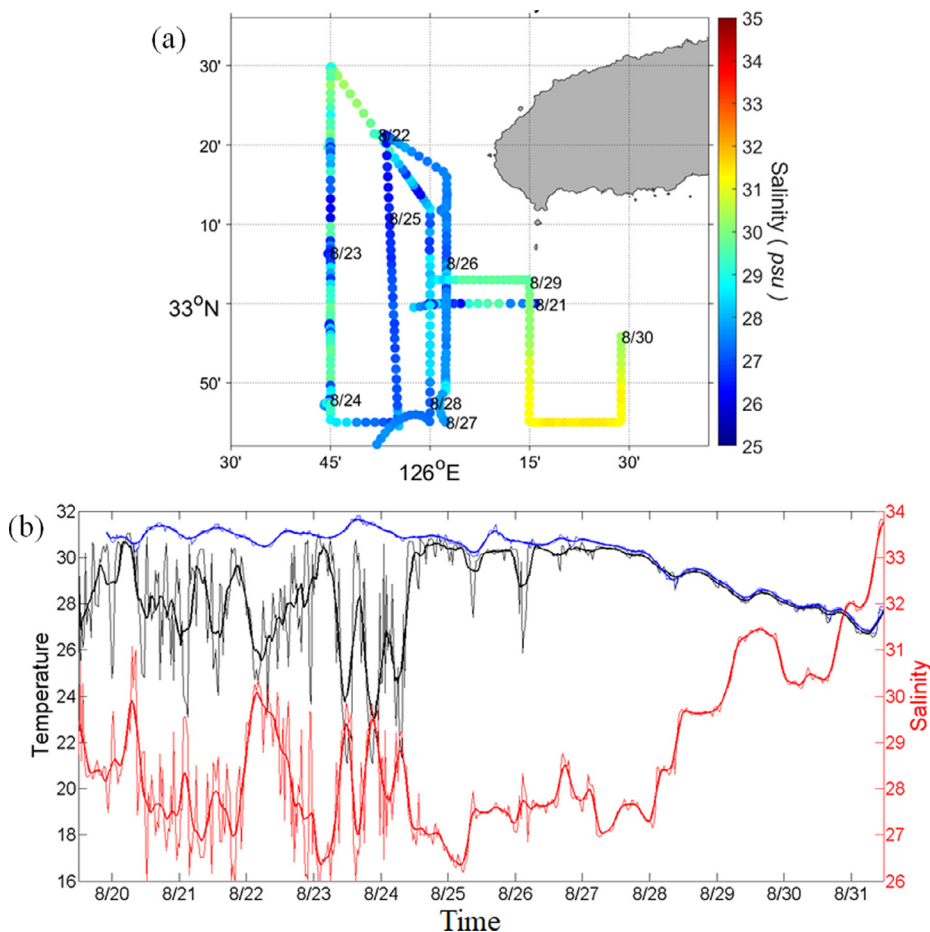
3. Abnormal low-salinity water observed during the summer of 2016

3.1. Sea surface freshening induced by CD in the northern ECS shelf

Vertical sections of salinity and temperature along the north-south KMA line (Fig. 2b) on late July 2016 are presented in Fig. 3. Low-salinity water (< 27 psu) clearly appeared near 32.5°N in the northeastern edge of the Changjiang Bank (CB) confined to depths less than 10 m, showing a shallow halocline in the surface layer. In contrast, relatively saline water (> 33 psu) was observed on the northeastern bottom slope of the CB, resulting in saline stratification between the upper and lower layers. The abnormal, low-salinity water can be attributed to the eastward extension of the CDW during June–July 2016, when the CD was substantially increased (Fig. 2c). Due to severe flooding in the Changjiang watershed during the summer of 2016, the discharge at Datong station reached its maximum of about $6.5 \times 10^4 \, \mathrm{m^3 \, s^{-1}}$ in July, which corresponds to an increase of ~40% relative to the average over the past decade. It is expected that the substantial volume of freshwater discharged from the Changjiang spreads offshore to the northeast of the CB during July, which is consistent with the typical path of the CDW. This pathway has been previously observed by Lie et al. (2003) who have shown that floats deployed near the Changjiang mouth traveled northeast across the CB before reaching the western sea of Jeju Island.

Due to surface heating in the summer, the water column was also well-stratified with a strong thermocline between the upper and lower layer (Fig. 3b). Warm water, with temperatures above 20 °C, appeared in the upper 20 m, whereas the bottom layer contained cold water, with temperatures below 12 °C. This pattern was distributed southward from the southern YS to the southwest of Jeju Island. This cold water

indicates the southward expansion of the YS bottom cold water in summer (Pang et al., 2003; Moon et al., 2009). An interesting thing is that warm surface water with temperatures above 26 °C was mainly detected over the northeastern shelf of the CB, wherein the strong and shallow halocline induced by the extension of the CDW was formed. This surface warming is fairly consistent with that observed in the SST anomalies for July, as observed by satellite measurements (Fig. 1a).

Temperature and salinity in the adjacent seas of Jeju Island observed by JNU on August 16–19, 2016, were used to identify the horizontal and vertical structures in the areas wherein substantial surface freshening occurred (Fig. 4). Abnormally low-salinity and high temperature water (< 26 psu, > 30 °C) appeared predominantly from the southwest to the north of Jeju Island (i.e., the Jeju Strait) along the Cheju Warm Current (CWC), which flows through the Jeju Strait after turning clockwise around Jeju Island (Lie et al., 2003). It is likely that the CDW observed around the northeastern CB moved northeastward to Jeju Island between late July and mid-August, maintaining its low salinity. The low-salinity water, restricted to the surface layer above 5 m depth, intruded farther eastward, exhibiting a salinity-induced ML depth that gradually increased from the west to the east (Fig. 4c). Because of the intrusion of the CDW, the low-salinity water was dominant in the upper layer, whereas the high-salinity water (> 34 psu) in the lower layer was distributed to the southeast of the Jeju Island. During the observation period, sea surface warming occurred over the entire survey area, except for the area to the east of Jeju Island. In particular, water with a high temperature above 31 °C appeared to the southwest of Jeju Island wherein the surface salinity was the lowest (Fig. 4a, b). In the lower layer, water with a temperature below 14 °C appeared to the southwest of Jeju Island with a strong and shallow thermocline at a depth of approximately 10–20 m (Fig. 4d). The thermocline sloped down toward the east, indicating a deeper thermocline depth into the
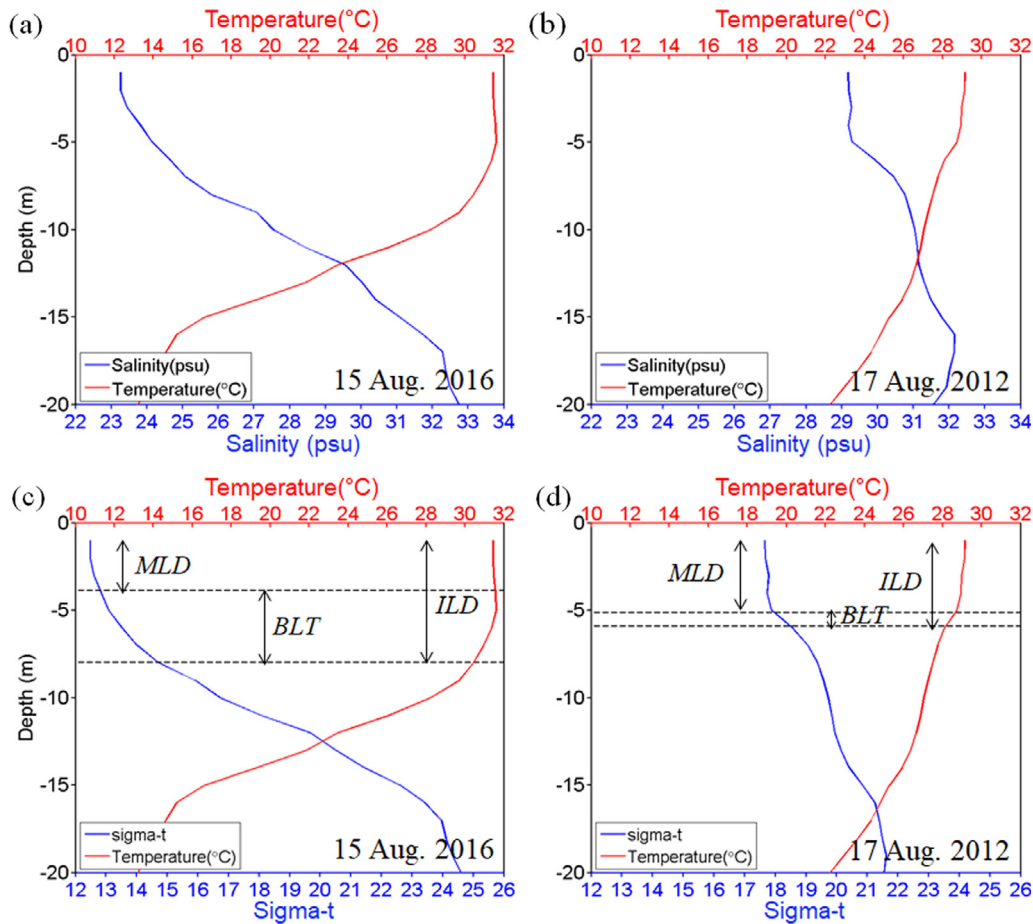
Fig. 6. Vertical profiles of (a, b) temperature and salinity and (c, d) temperature and density at a location off the west coast of Jeju Island, marked by red dot in Fig. 2b, in August 2016 and August 2012. (For interpretation of the references to colour in this figure legend, the reader is referred to the web version of this article.)

Table 1
RMSEs and correlations of harmonic constants to the tide gauge measurements.

		M_2	S_2	K_1	O_1
Amplitude (cm)	RMSE	11.8	6.0	2.7	3.4
	Corr.	0.99	0.98	0.89	0.55
Phase (°)	RMSE	11.7	10.6	8.1	7.8

southeast of Jeju Island. This suggests a mixing process among three types of water masses in the seas adjacent to the Jeju Island: the intruded CDW with its high temperature surface layer, the cold and less saline water extending from the southern YS, and the warm and saline ECS water carried by the CWC to the Korea/Tsushima Strait.

3.2. Formation of near-surface ML and BL in low-salinity areas

The intrusion of low-salinity water was also evident from the salinity data at a depth of 8 m along the track of a wave-glider-mounted CTD (Fig. 5). During the tracking periods on August 21–30, 2016, the salinities show large spatial variation with a range from 26 to 31 psu (Fig. 5a). Low-salinity (< 29 psu) conditions were mostly distributed to the southwest of Jeju Island, whereas the recorded salinity increased toward the east, as the glider left the low-salinity areas. When the glider traveled around the freshening areas, the salinity measured at a depth of 8 m varied sharply with time, with a range exceeding 3 psu (Fig. 5b). The sharp variations in salinity continued until August 27, and thereafter the salinity gradually increased with time. The temperature measured at a depth of 8 m also varied in a way similar to the salinity

(Fig. 5b) but the signal is essentially opposite. Unlike the subsurface temperature, the SST measured by the glider-mounted ADCP had a diurnal variation, with high temperatures ranging from 31 °C to 32 °C (Fig. 5b), thereby producing the large temperature difference between the surface and subsurface layers. The contrasts between the temperature and salinity patterns can be explained by internal waves in the stratified density structure at the interface between the warm/fresh surface water and the cold/saline subsurface water. The observations provided by the glider imply that a very sharp density change occurred along the interface, and therefore a shallow ML formed in the low-salinity areas. However, the sharp increase and decrease in subsurface temperature and salinity measurement disappeared almost entirely after August 28, 2016, when the glider moved eastward to the south of Jeju Island. Both the surface and the subsurface temperatures decreased gradually with time, while the subsurface salinity increased concurrently, indicating that the ML became thick when the glider was out of the freshening areas.

Analysis of the glider data suggested the formation of a strong vertical salinity gradient that led to a very shallow mixed layer across the freshening areas, in which the most significant warming of SSTs was found. Near-surface salt stratification can lead to BL formation between the base of the ML and the top of the thermocline. To identify the relationship between the shallow salinity-stratified ML and BL formation, we compared the *in situ* ocean profiles observed in August 2016 with those from August 2012 when no significant surface freshening was recorded (Fig. 6). The CTD measurements for the two years were conducted at one station near the west coast of Jeju Island (Fig. 2b). Herein, the ML depth (MLD) can be estimated based on density variation ($\Delta\sigma_t$) determined from the corresponding temperature change (ΔT)
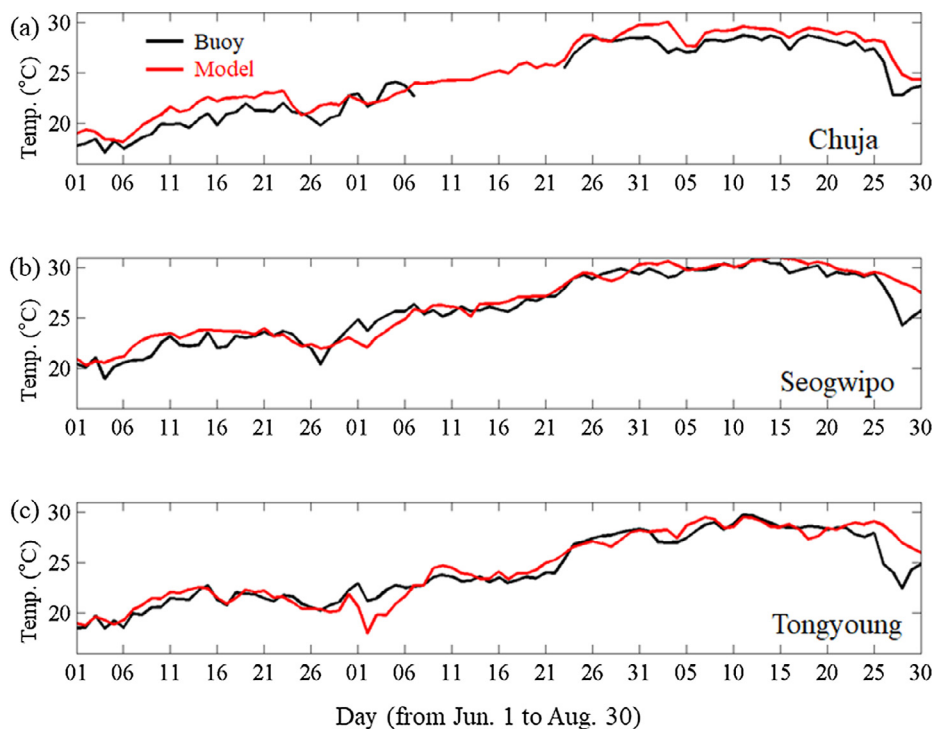
Fig. 7. Comparison of modeled surface temperature with observations at three ocean buoys, (a) Chuja, (b) Seogwipo, and (c) Tongyoung, from the period of June to August 2016. The ocean buoys are shown in Fig. 2b with red-asterisk symbols. (For interpretation of the references to colour in this figure legend, the reader is referred to the web version of this article.)
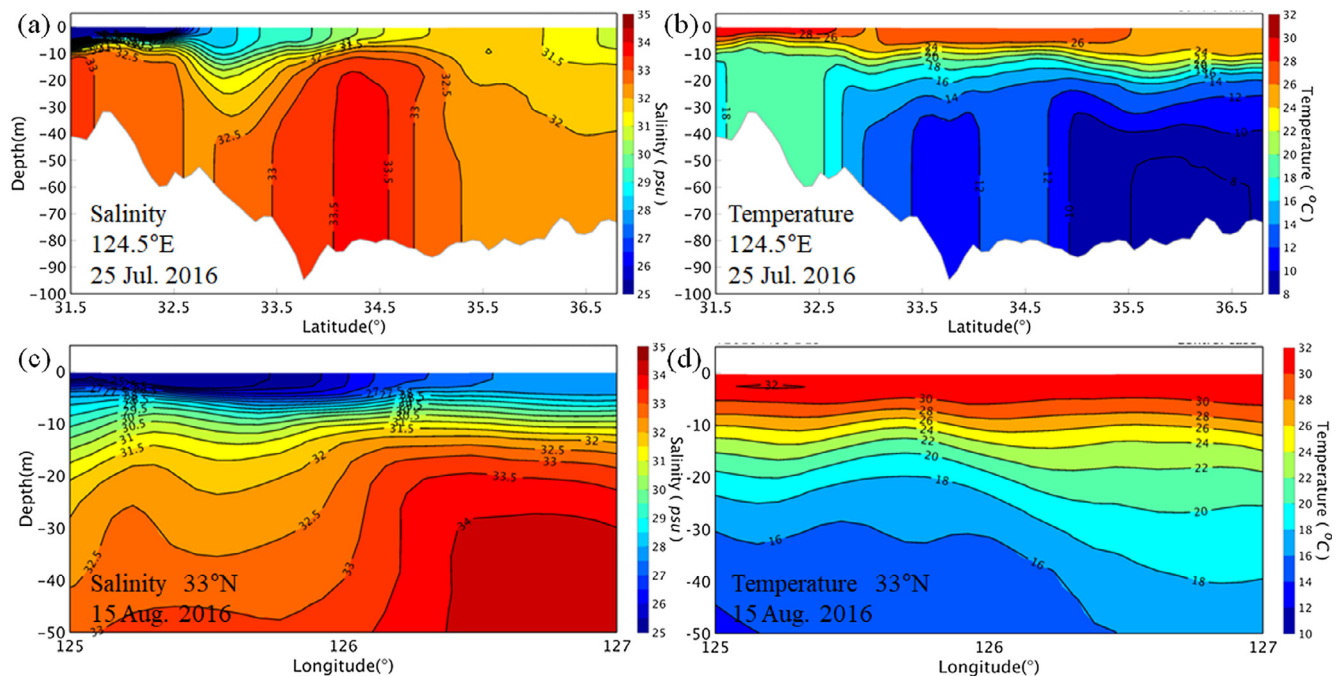
Fig. 8. Vertical sections of simulated (a, c) salinity and (b, d) temperature along 124.5°E and 33°N, which correspond to the KMA and JNU observation lines.

using the equation of state (e.g., Kara et al., 2000; Vissa et al., 2012).

$$\Delta\sigma_t = \sigma_t(T + \Delta T, S, P) - \sigma_t(T, S, P) \qquad (1)$$

A temperature decrease of 1 °C was chosen to estimate the MLD. The depth of IL (ILD), which represents the top of the thermocline, can be defined as the depth at which the temperature decreases to a value 1 °C lower than the SST. During the summer of 2016, the freshwater associated with the CDW intrusion was confined to a thin surface layer shallower than 10 m and maintained a strong vertical salinity gradient (Fig. 6a). The corresponding density profile indicates that the salinity gradient directly controlled the near-surface density stratification,

thereby forming a very shallow surface ML in which temperatures exceeded 31 °C (Fig. 6c). To summarize, the shallow ML induced by the fresh water of the CDW led to the formation of a BL, which is defined by the difference between the ILD and MLD. In contrast, when no low-salinity water (< 29 psu) was found, as was the case in 2012, the difference between the two layers was correspondingly narrower (Fig. 6d). These results demonstrate that the CDW contributes to the enhancement of BL thickness (BLT) by inducing a near-surface salinity-stratified ML to be well separated from the thermocline. Considering that an enhanced BL restricts the vertical heat exchange, the SST warming can be enhanced by trapping heat in the shallow ML (Park et al., 2011). The
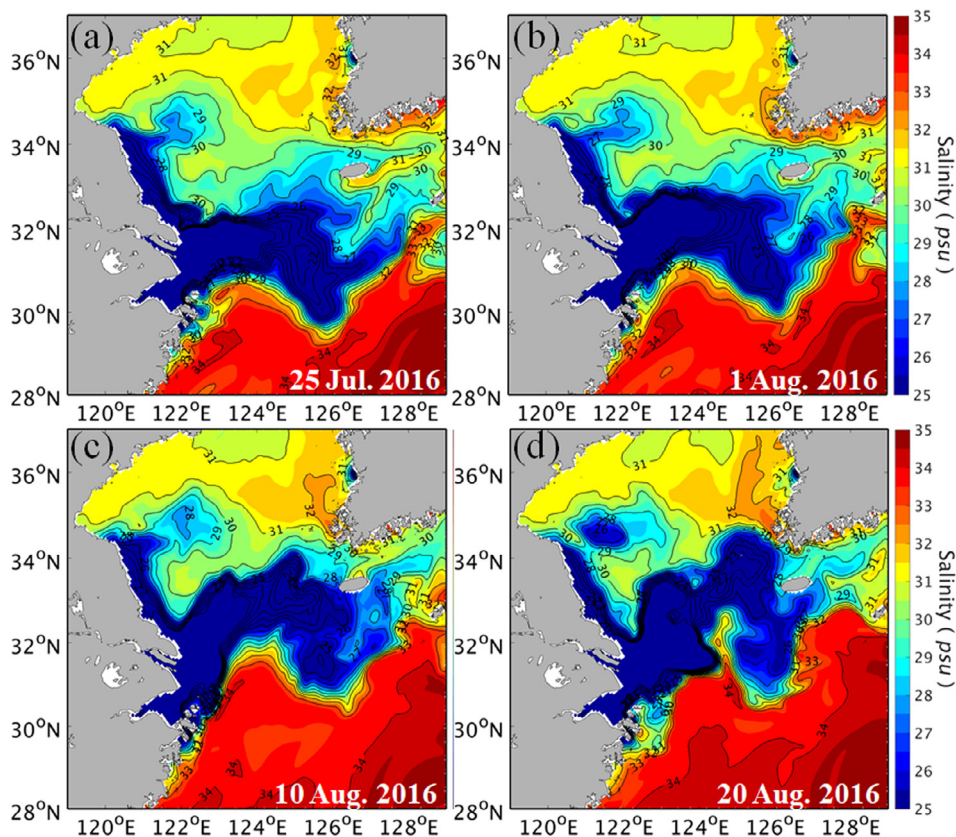
Fig. 9. Horizontal distributions of simulated salinity in the surface layer from July 25 to August 20, 2016.

warming response to the CDW using the two comparative experiments will be discussed in the following subsections.

4. Contribution of sea surface freshening to SST warming

4.1. Simulated significant surface freshening

Before proceeding to a comparison of the two simulations, we need to confirm that the model with the CD at zero salinity yielded acceptable results. First, the harmonic constants of four major tidal constituents derived from the model output were compared with those derived from several tide gauge stations, wherein the red-cross symbols are depicted in Fig. 2a. As listed in Table 1, the simulated harmonic constants (amplitude and phase of M_2, S_2, K_1 and O_1) are in very good agreement with those estimated from the observations, with statistically significant correlation coefficients exceeding 0.9 except for the amplitude of O_1. The modeled surface temperature change was also validated by direct observations collected at three ocean buoys (red asterisk symbols in Fig. 2b) from the period of June to August 2016 (Fig. 7). The simulated surface temperature at three buoy stations matches well with the observations throughout the time series, with the root-mean-square error all less than 0.65 °C.

Simulated vertical sections of salinity and temperature along the north-south KMA line at 124.5°E and the east-west JNU line at 33°N are presented in Fig. 8. Compared with the observed data (Figs. 3 and 4), our hindcast simulation adequately reproduced the vertical salinity and temperature structures. For example, the modeled and observed data characterize the surface water as being warm and containing low salinity because of the extension of the CDW into the northern ECS shelf. The low-salinity water (< 28 psu) was restricted to near-surface water (above 5 m depth), whereas more saline water (> 33 psu) was widely distributed in the lower layer. In particular, the model successfully captured the sea surface warming over the substantial freshening areas.

From late July to early August, the freshwater plume extended eastward from the river mouth to the central ECS, as a broad tongue-shaped pattern pushed by an ambient current, which entered the southern flank off the Changjiang along the 50 m isobaths (Fig. 9a, b). Thereafter, substantial portions of the freshwater moved northeastward to the western region of Jeju Island and reached the southeastern YS, forming broad surface freshening areas over the northern ECS (Fig. 9c, d). To identify a thermal response to the surface freshening, temporal changes in salinity and temperature at the northern ECS (at a location of 124.5°E and 32°N) are presented in Fig. 10. The low-salinity water less than 28 psu started to appear from early July and then sharply decreased its value from mid-July to early August, which corresponds to the eastward extension of the CDW mentioned above. The salinity reached its minimum value from late July, thereby causing the strong salinity stratification in the surface layer. The surface temperature increased gradually in time, with the highest temperature occurred from late July which corresponds the time when the extremely low-salinity was observed in the surface layer.

4.2. Warming response to salinity-induced BL formation

To gain further insight into the role of the CDW on SST warming with relation to BL formation, a comparison was made between the two simple model configurations: one with the CD at zero salinity and the other with the CD at 30 psu. Fig. 11 shows the differences in surface salinities and temperatures between the two experiments on late July and mid-August 2016. The negative (positive) values indicate decreases (increases) in salinity and temperature when the CD at zero salinity value was applied into the model. Not surprisingly, well-defined negative salinity anomalies were identified over the northern ECS shelf, which is consistent with the results of a previous study (Park et al., 2011). A large amount of the flooding-associated fresh water was discharged into the ECS, thereby producing substantial volumes of low-
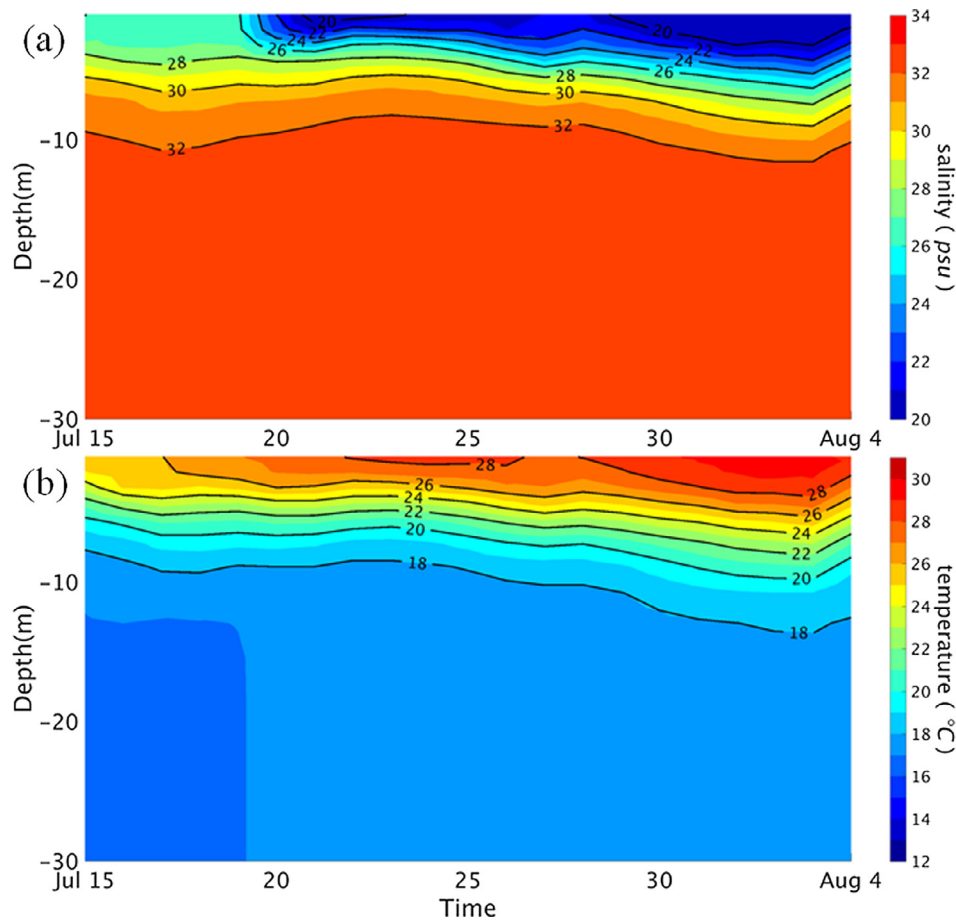
Fig. 10. Depth-time diagram for modeled (a) salinity and (b) temperature at a location of 124.5°E and 32°N from July 15 to August 4, 2016. The contour intervals are 2 psu and 1 °C for salinity and temperature, respectively.

salinity water by mixing with saline ambient water. The CDW spread offshore from the river mouth toward Jeju Island, resulting in enhanced surface freshening over the northern ECS shelf regions. Significant surface warming anomalies were clearly detected over the central and northern ECS regions (Fig. 11c, d). On late July, a strong warming area appeared from the river mouth toward the central ECS, extending northeastward to the west side of Jeju Island. The strong warming signals mostly correspond to the regions with significant freshening. The connection between SST increase and surface freshening is also evident in Fig. 12, which shows the vertical differences in salinity and temperature between the two experiments along two lines at 32°N and 33°N (Fig. 11c, d). In both transects, strong negative salinity was clearly confined to a thin surface layer shallower than ~5 m in depth, which corresponds to positive temperature anomalies with strong vertical temperature gradients. Below these layers, the models revealed a boundary layer that separates the surface from the subsurface negative temperature anomalies. These results suggest that additional freshwater influx creates a shallower salinity-induced ML, which in turn leads to a formation of a BL between the ML and the layer below the ML. Because of the BL formation, near-surface water becomes warmer, whereas the water below the ML becomes colder when the surface freshening is more intensive. In addition, the subsurface cold water below the ML directly contributes to the rate of surface cooling along the slope off the Subei coast (see Fig. 12c,d), wherein tide-induced vertical mixing is dominant (Yuan et al., 2017). This cooling anomaly off the Subei coast has also been reported by Kako et al., 2016) who compared the ocean circulation model results with and without the CD. To more examine the contribution of mixing for responsible for the surface warming, the vertical diffusion term ($\partial_z(k_z\partial_z T)$, with k_z being the vertical diffusion

coefficient) in temperature rate equation was compared between the two comparative experiments (Fig. 13). When the CD at zero salinity was applied, strong vertical diffusion was only restricted to near-surface layer in both of the two sections (Fig. 13a, b), suggesting that the vertical exchange can be restricted to only the shallow ML. On the other hand, the vertical diffusion can reach the top of the thermocline when the CD at 30 psu was applied into the model (Fig. 13c, d). The comparison indicates that the low salinity-induced ML to be separated from the thermocline can enhance the BL formation, thereby contributing to the warming at the surface layer.

To examine the BL formation associated with surface freshening, the salinity-induced BL between the two comparative model results are presented in Fig. 14. The most pronounced response to stronger surface freshening was the thickening of the BL over the central and northern ECS shelf regions, which corresponds to the regions wherein the surface warming was robust. This result indicates that the SST warming associated with the surface freshening is accompanied by enhanced BL formation, which is consistent with the observations mentioned above. Temporal changes in BL formation during the two model tests, sampled from a location of 124.5°E and 32°N, were used to compare the responses of BL thickness to surface freshening (Fig. 15). As expected, the surface freshening clearly developed the very shallow MLD and relatively thick BL, and the maximum BLT occurred from early August when the surface freshening was robust. In contrast, when the freshening is not intensive, the salinity-induced ML is deeper and the BL is thinner compared to the results of significant surface freshening. These comparisons demonstrate that the salinity-stratified ML has a profound impact on the enhancement of BL formation that leads to enhanced SST warming over the areas wherein the surface freshening is significant.
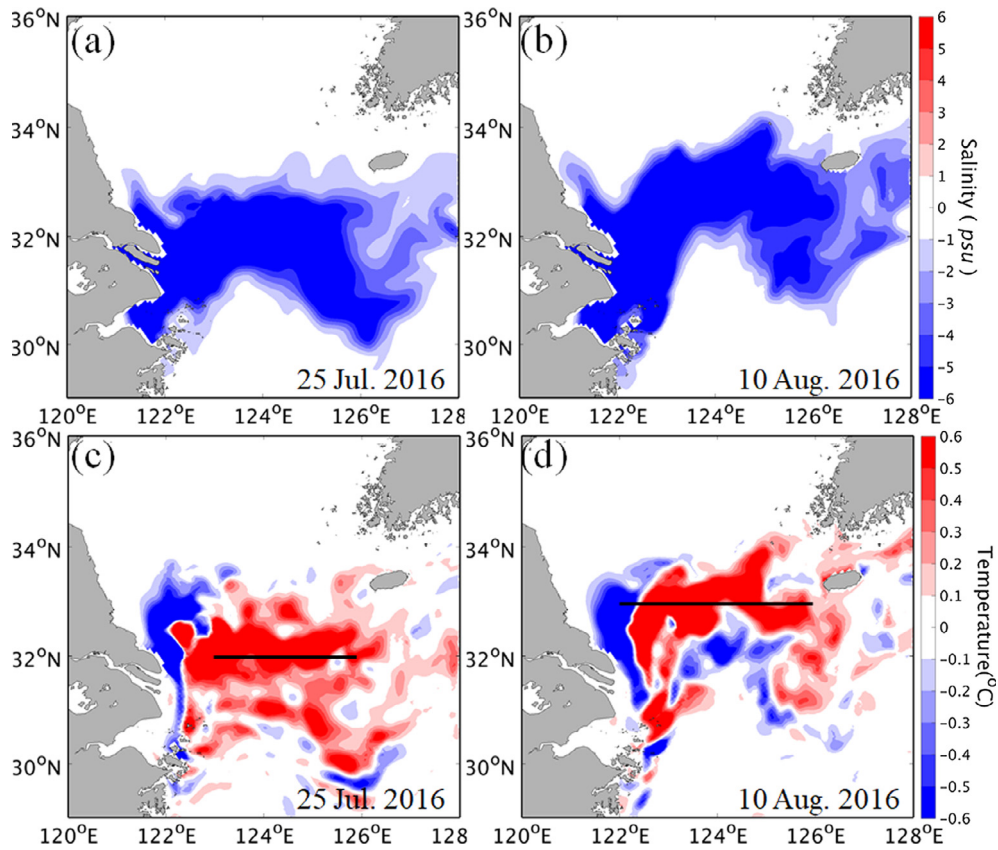
Fig. 11. Spatial patterns of model differences in (a, b) salinity and (c, d) temperature between the two experiments with zero and 30 psu salinity as a river source on July 25 and August 10, 2016.
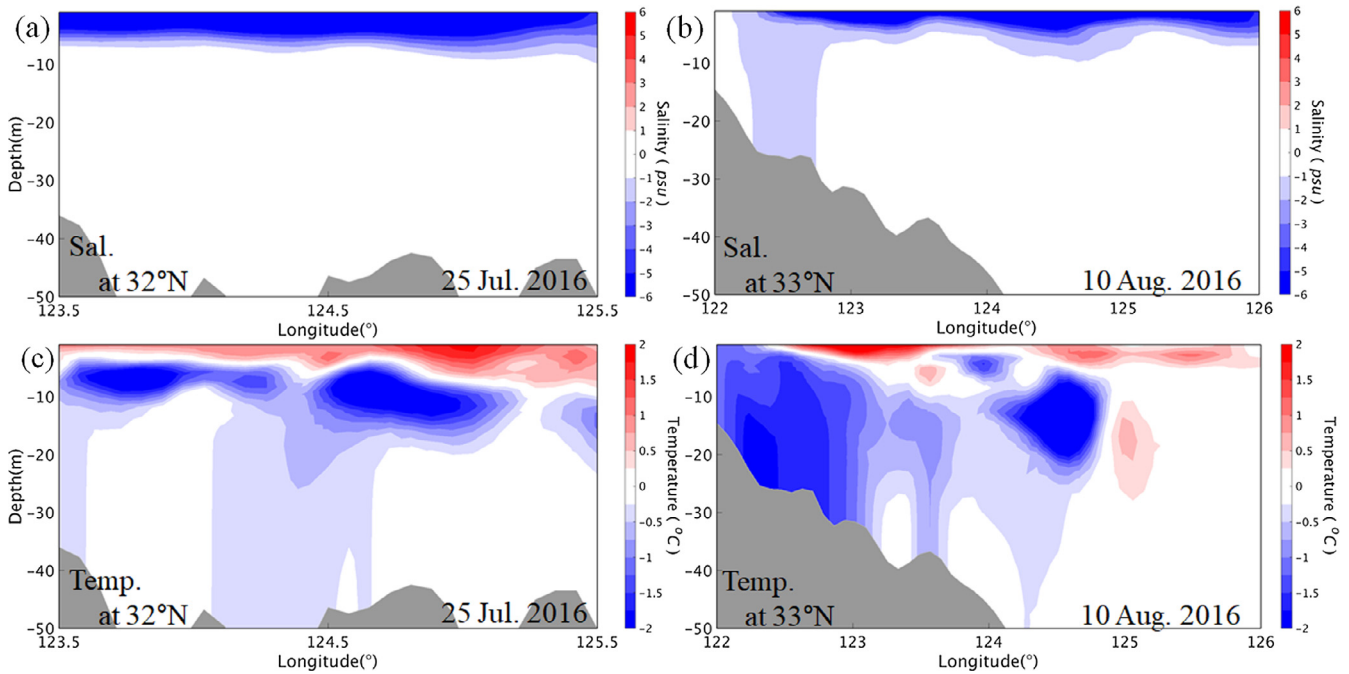
Fig. 12. Vertical sections of model differences in (a, b) salinity and (c, d) temperature between the two experiments with zero and 30 salinity as a river source along 32°N and 33°N on July 25 and August 10, 2016. The vertical lines are shown in Fig. 11c and 11d, respectively.

5. Summary and discussions

Satellite-derived SST measurements showed a significant warming anomaly over the northern ECS shelf regions during the summer of 2016, which was a phenomenon rarely observed over the past decade, which caused severe damage to the fishing and aquaculture industries in Korea. By analyzing the ship-based hydrographic data, the horizontal temperature and salinity distributions tracked by a wave glider, and the
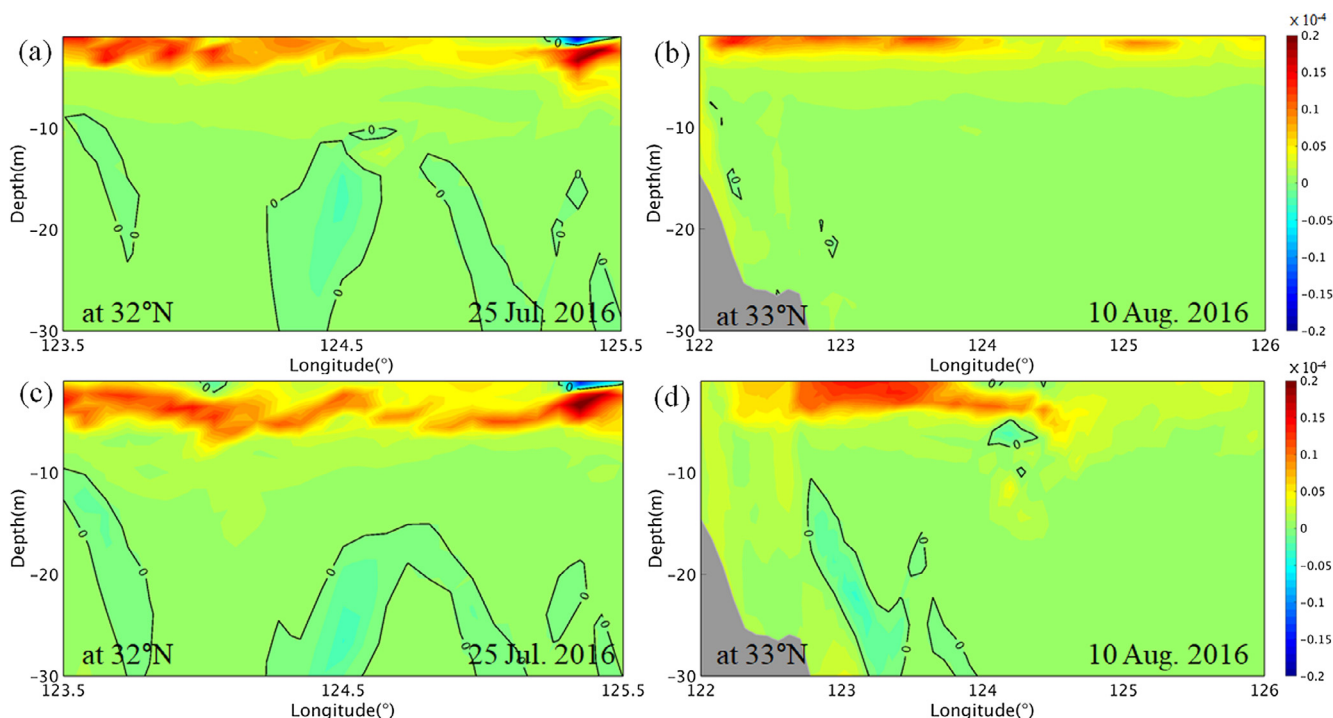
Fig. 13. Vertical sections of vertical diffusion term (°C/s) in temperature rate equation along 32°N and 33°N on July 25 for the two experiments with (a, b) zero and (c, d) 30 salinity as a river source and August 10, 2016.
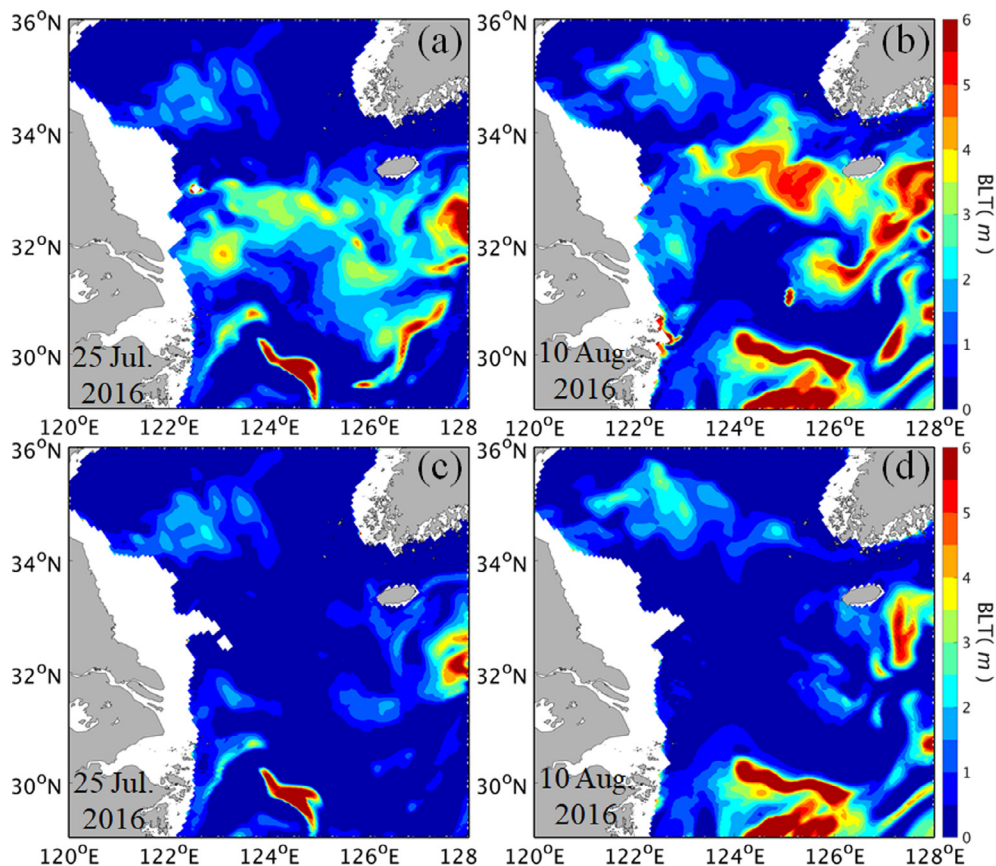
Fig. 14. Spatial patterns of barrier layer thickness for the two experiments with (a, b) zero and (c, d) 30 salinity as a river source on July 25 and August 10, 2016.

results from a regional ocean model, this study investigated the spatiotemporal behavior of the CDW and its contribution to sea surface warming over the northern ECS. The observations indicate the formation of a very shallow surface ML during summer in which strong SST warming was observed. This shallow ML resulted from CD-induced salinity stratification and led to BL formation between the ML and the
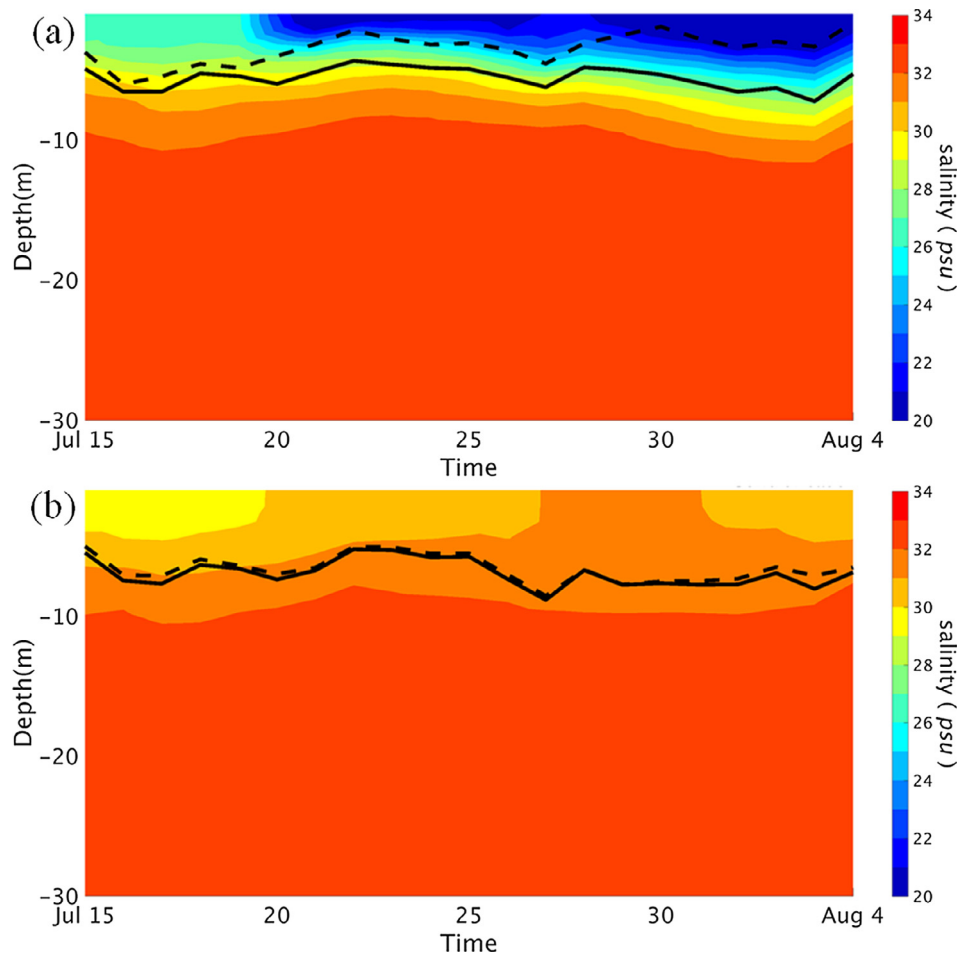
Fig. 15. Depth-time diagram of salinity with the mixed layer depth (MLD, dashed line) and isothermal layer depth (ILD, solid line) for the two experiments with (a) zero and (b) 30 salinity as a river source, at a location of 124.5˚E and 32˚N from July 15 to August 4, 2016.

layer below ML. Because this enhanced BL impedes vertical heat exchange between the warm surface and the cold thermocline below, the sea surface warming was enhanced where surface freshening occurred. Our model successfully captured the strong surface warming over the northern ECS, as observed during the summer of 2016. The SST warming associated with the surface freshening was also accompanied by enhanced BL formation. To confirm the role of the CDW on the SST warming with relation to BL formation, we compared the results between two model configurations with no salinity and 30 psu as the salinity of the river source. The comparisons demonstrate that the salinity-stratified ML has an important impact on the enhancement of BL formation, which in turn led to enhanced SST warming over the areas where surface freshening was robust.

The surface warming associated with the salinity-induced BL has implications for regional and local weather systems through ocean-atmosphere interactions. For example, broad increases in SST may lead to the production of relatively warm air masses in the ECS that may move across the Korean Peninsula. The significant warming can also affect the intensity of typhoons, as mentioned by Park et al. (2011). Although not investigated in this study, the potential impacts of salinity-stratified BLs on regional weather forecasting would be an interesting subject for future work.

References

Bleck, R., 2002. An oceanic general circulation model framed in hybrid isopycnic-Cartesian coordinates. Ocean Model. 4 (1), 55–88.

Chapman, D.C., 1985. Numerical treatment of cross-shelf open boundaries in a barotropic coastal ocean model. J. Phys. Oceanogr. 15 (8), 1060–1075.

Chassignet, E.P., Hurlburt, H.E., Smedstad, O.M., Halliwell, G.R., Hogan, P.J., Wallcraft, A.J., Bleck, R., 2007. The HYCOM (hybrid coordinate ocean model) data assimilative system. J. Marine Syst. 65 (1), 60–83.

Chang, P.-H., Isobe, A., 2003. A numerical study on the Changjiang diluted water in the Yellow and East China Seas. J. Geophys. Res. 108, 3299. https://doi.org/10.1029/2002JC001749.

Daniel, T., Manley, J., Trenaman, N., 2011. The Wave Glider: enabling a new approach to persistent ocean observation and research. Ocean Dyn. 61, 1509–1520. https://doi.org/10.1007/s10236-011-0408-5.

Delcroix, T., Murtugudde, R., 2002. Sea surface salinity changes in the East China Sea during 1997–2001: Influence of the Yangtze river. J. Geophys. Res. 107, 8008. https://doi.org/10.1029/2001JC000893.

Fairall, C.W., Bradley, E.F., Rogers, D.P., Edson, J.B., Young, G.S., 1996. Bulk para-meterization of air-sea fluxes for tropical ocean-global atmosphere coupled-ocean atmosphere response experiment. J. Geophys. Res. 101 (C2), 3747–3764.

Foltz, G.R., McPhaden, M.J., 2009. Impact of barrier layer thickness on SST in the central tropical north Atlantic. J. Clim. 22, 285–299.

Gao, H., Yang, S., Kumar, A., Hu, Z.Z., Huang, B.H., Li, Y.Q., Jha, B., 2011. Variations of the East Asian Mei-yu and simulations and prediction by the NCEP Climate Forecast System. J. Clim. 24, 94–108. https://doi.org/10.1175/2010JCLI3540.

Haidvogel, D.B., Arango, H., Budgell, W.P., Cornuelle, B.D., Curchitser, E., Di Lorenzo, E., Levin, J., 2008. Ocean forecasting in terrainfollowing coordinates: Formulation and skill assessment of the Regional Ocean Modeling System. J. Comput. Phys. 227 (7), 3595–3624.

Hong, J.S., Moon, J.H., Lee, J.H., Pang, I.C., 2016. Modeling the largest inflow of Changjiang freshwater into the Yellow Sea in 2012 with particle-tracking experiment. Ocean Sci. J. 51 (4), 549–562.

Kako, S., Nakagawa, T., Takayama, K., Hirose, N., Isobe, A., 2016. Impact of Changjiang River Discharge on sea surface temperature in the East China Sea. J. Phys. Oceanogr. 46, 1735–1750.

Kara, A.B., Rochford, R.A., Hurlburt, H.E., 2000. An optimal definition for ocean mixed layer depth. J. Geophys. Res. 105, 16803–16821.

Lee, J.H., Pang, I.C., Moon, J.H., 2016. Contribution of the Yellow Sea bottom cold water to the abnormal cooling of sea surface temperature in the summer of 2011. J. Geophys. Res. Oceans 121, 3777–3789. https://doi.org/10.1002/2016JC011658.

Lie, H.J., Cho, C.H., Lee, J.H., Lee, S., 2003. Structure and eastward extension of the Changjiang River plume in the East China Sea. J. Geophys. Res. 108, 3077. https://doi.org/10.1029/2001jc001194.

Lukas, R., Lindstrom, E., 1991. The mixed layer of the western equatorial Pacific ocean. J. Geophys. Res. 96, 3343–3358.

Marchesiello, P., McWilliams, J.C., Shchepetkin, A., 2001. Open boundary conditions for long-term integration of regional oceanic models. Ocean Model. 3 (1), 1–20.

Moh, T., Cho, J.H., Jung, S.-K., Kim, S.-H., Son, Y.B., 2018. Monitoring of the Changjiang River Plume in the East China Sea using a Wave Glider. J. Coast Res. SI (85), 26–30.

Moon, J.H., Pang, I.C., Yoon, J.H., 2009. Response of the Changjiang diluted water around Jeju Island to external forcings: A modeling study of 2002 and 2006. Cont. Shelf Res. 29, 1549–1564. https://doi.org/10.1016/j.csr.2009.04.007.

Moon, J.H., Hirose, N., Yoon, J.H., Pang, I.C., 2010. Offshore detachment process of the low-salinity water around Changjiang Bank in the East China Sea. J. Phys. Oceanogr. 40, 1035–1053.

Moon, J.H., Hirose, N., Pang, I.C., Hyun, K.H., 2012. Modeling offshore freshwater dispersal from the Changjiang River and controlling factors during summer. Terr. Atmos. Ocean Sci. 23, 247–260.

Pang, I.C., Hong, C.S., Chang, K.I., Lee, J.C., Kim, J.T., 2003. Monthly variation of water mass distribution and current in the Cheju Strait. J. Korean Soc. Oceanogr. 38 (3), 87–100.

Park, T., Jang, C.J., Jungclaus, J.H., Haak, H., Park, W., Oh, I.S., 2011. Effects of the Changjiang river discharge on sea surface warming in the Yellow and East China Seas in summer. Cont. Shelf Res. 31, 15–22. https://doi.org/10.1016/j.csr.2010.10.012.

Senjyu, T., Enomoto, H., Matsuno, T., Matsui, S., 2006. Interannual salinity variations in the Tsushima Strait and its relation to the Changjiang discharge. J. Oceanogr. 62, 681–692.

Shen, H., Zhang, C., Xiao, C., Zhu, J., 1998. Change of the discharge and sediment flux to estuary in Changjiang River. In: Hong, C.H. (Ed.), Health of the Yellow Sea. Earth Love, Seoul, pp. 129–148.

Sprintall, J., Tomczak, M., 1992. Evidence of the barrier layer in the surface-layer of the tropics. J. Geophys. Res. 97, 7305–7316.

Shchepetkin, A., McWilliams, J.C., 2005. The regional oceanic modeling system (ROMS): A split-explicit, free-surface, topographyfollowingcoordinate oceanic model. Ocean Modell. 9 (347), 404. https://doi.org/10.1016/j.ocemod. 2004.08.002.

Umlauf, L., Burchard, H., 2003. A generic length-scale equation for geophysical turbulence models. J. Mar. Res. 61 (2), 235–265.

Vissa, N.K., Satyanarayana, A.N.V., Kumar, B.P., 2012. Comparison of mixed layer depth and barrier layer thickness for the Indian Ocean using two different climatologies. Int. J. Climatol. https://doi.org/10.1002/joc.3635.

Warner, J.C., Sherwood, C.R., Butman, B., Arango, H.G., Signell, R.P., 2005. Performance of four turbulence closure models implemented using a generic length scale method. Ocean Model. 8, 81–113.

Yuan, D., Li, Y., Wang, B., He, L., Hirose, N., 2017. Coastal circulation in the southwestern Yellow Sea in the summer of 2008. Cont. Shelf Res. 143, 101–117.